THE PROPAGATION OF STABLE RADIO FREQUENCY SIGNALS THROUGH THE ATMOSPHERE

Charles Naudet, Christopher Jacobs, Steve Keihm, Gabor Lanyi, George Resch, Lance Riley, Hans Rosenberger, Alan Tanner

Abstract

The terrestrial troposphere and ionosphere are known to have strong effects on the radiation fields traversing them. The primary types of effects are refraction (deflection, polarization rotation, propagation velocity changes), absorption, and scattering by the turbulent structure in the media. In particular, the wet troposphere plays a very important role in precise radio propagation. The phase accuracy of VLBI measurements and spacecraft Doppler tracking at frequencies greater than 5 GHz is dominated by fluctuations in the distribution of water vapor.

The Deep Space Network is supporting the Gravitational Wave Experiment (GWE) on the Cassini spacecraft by providing atmospheric media calibration for precise Doppler tracking. The two-way communication link between the ground station and the Cassini spacecraft are in effect an "antenna" for gravitational waves that will perturb the phase of the RF signal between the Earth and the spacecraft. The experiment will be sensitive to gravitational wave perturbations larger than the noise level fluctuations of 3×10^{-15} as measured in the Allan Standard Deviation Domain.

We have designed and are testing a new atmospheric calibration system to sense line-of-sight water vapor and its physical temperature with a goal of calibrating 95% or more of water vapor fluctuation during the Cassini GWE. The calibration system consists of a newly designed water vapor radiometer having a 1 degree sensing beamwidth, a microwave temperature profiler to retrieve the vertical distribution of the vapor physical temperature, and surface meteorology. Two water vapor calibration systems have been constructed in order to provide side-by-side testing capability as well as backup during the actual experiment. We will report on an independent test of these calibrations systems done by comparing them to a short baseline radio interferometric measurement at our Goldstone complex.

Introduction

Over the last several years we have been involved in an effort to support the Cassini radio science experiments. The Cassini spacecraft was launched in 1997, will arrive at Saturn in 2004, and will start radio science experiments during its cruise phase (early 2001). These experiments extract interesting physical phenomena, such as the structure of planetary atmospheres and evidence of gravitational waves, by measuring the perturbations of the geometric delay along the line-of-sight to the spacecraft. The Cassini gravitational wave experiment (GWE) has been described in detail by Armstrong [1], and Tinto and Armstrong [2]. Detailed studies of the GWE error budget [3,4] point to the atmospheric delay fluctuations as the dominate component on time scales greater than 100 seconds. Thus the sensitivity of the GWE will be limited by the ability to calibrate out these atmospheric delay fluctuations. Since almost all the power in the atmospheric delay fluctuations at frequencies less than 0.01 Hz is due to the wet troposphere the principle instrumention used for calibration is a water vapor radiometer.

An advanced water vapor radiometer (WVR), shown in Figure 1, was developed at JPL and is described in detail by Tanner [5]. The WVR has an off-axis 1 meter diameter reflector that has a one degree beamwidth with .1 degree pointing accuracy. The WVR measures the brightness temperature at 22.2, 23.8, and 31.4 GHz with 10 mk of stability. The path delay along the line-of-sight is proportional to the integrated columnar content of water vapor which may be estimated by measuring the strength of the 22.2 GHz spectral line of water. However, this rotational transition is sensitive to pressure changes, it undergoes line broadening with increasing pressure. To compensate for the decrease in absorption at resonance an additional measurement at the half-power point (23.8 GHz) is made where the absorption increases with pressure. Finally, to remove the strong absorption of water droplets in clouds an additional measurement off-resonance (31.4 GHz) is chosen. In a quadratic combination with the on-resonance measurements the effect of clouds can be removed. The WVR acquires data in subsecond intervals and produces a time-series of brightness temperatures, azimuths, and elevations. Off to the right in the background of the picture one can see the microwave temperature profiler (MTP) and the early J-series WVR. The microwave temperature

profiler retrieves the vertical distribution of the vapor physical temperature. The data from the WVR, MTP, and surface meteorological stations are then post-processed with two retrieval algorithms [8,9] to extract the line-of-sight delay

Performance Testing

The objective of the Cassini media calibration system is to measure the atmospheric path delay fluctuation of signals transmitted between the Cassini spacecraft and the Goldstone DSS-25 antenna. Two advanced WVRs have been built to support the experiment. This allows for operational reliability and robustness in the case of one units failure and allows cross-checks between the units. A detailed intercomparison between the two unit has been made, see [5], and the Allan standard deviation [10] was shown to be significantly better than the GWE requirements for all interval times greater than 100 seconds. However, this side-by-side comparison reflects only the stability of the WVR in order to demonstrate it's accuracy its necessary to calibrate it to another measurement technique. Following earlier successful comparison experiments [6,7] a connected element interferometer (CEI) was used to independently measure the line-of-sight path delay fluctuations. A overview of the experimental setup is shown in Figure 2.

From Aug, 1999 until May, 2000 we have conducted a series of dual frequency (2.3 and 8.4 GHz) CEI observations on the 21 km baseline between the Deep Space Networks (DSN) high efficiency 34m diameter antenna at DSS-15 and a 34 m diameter beam waveguide antenna at DSS-13. Since the effective wind speed is typically less than 5-10 m/s the tropospheric fluctuations at each site will be independent for time scales less than ~4000 seconds making this baseline well-suited for a WVR comparison experiment. Strong, point-like radio quasar sources (S > 1 Jy) with very accuracy positions were chosen to minimize CEI errors. The S and X band data from each antenna is cross-

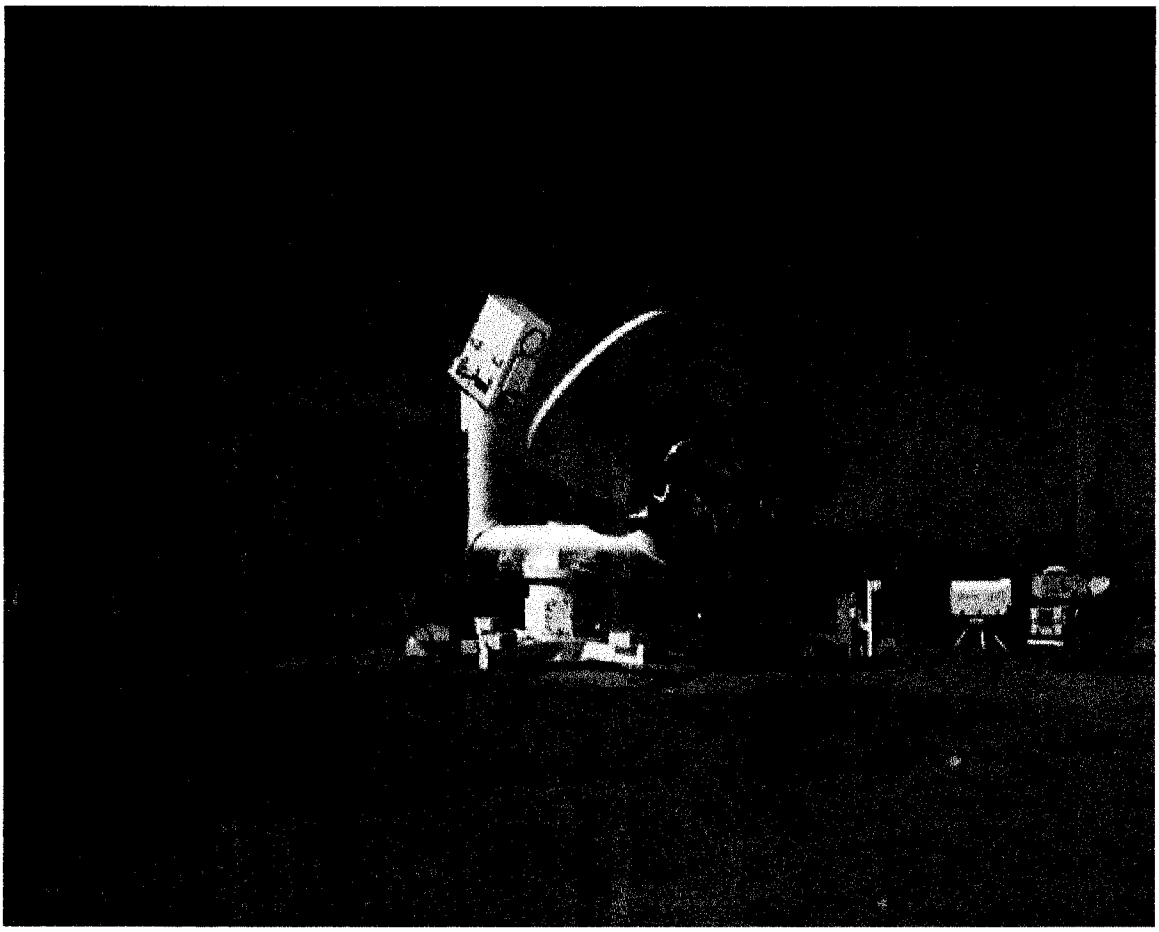

Figure 1. A photo of the Cassini Calibration Subsytem taken at DSS-13 in Goldstone CA. The new advanced WVR is seen in the center and the MTP and J-series WVR are shown in the background to the right.

correlated and the geometric delay is extracted. After subtraction of an accurate model, the residual phase delay and delay rate are produced. In addition, the fringe fitting model [11] linearly detrends the phase delay removing any clock-like effects.

Each WVR was positioned ~50 meters from the base of the 34m antenna which maximized the sky coverage yet minimized the effects of beam-offset and beam shape mismatch [12,13]. The WVR was co-pointed with the DSN antennas. The WVRs were monitored in real time and the path-delay time series were produced during post-processing at JPL. After the WVR path delay time series were smoothed over 6 seconds the WVR data from each site (DSS-15, DSS-13) were subtracted to create a site-differenced phase delay time-series. Finally, the data was linearly detrended, removing clock-like effects, resulting in a differenced WVR data type which can be directly compared with the CEI residual phase delay.

The comparison experiments conducted in 1999 were limited in scan duration to less than 26 minutes (the duration of a single pass on the CEI tape recorder). However, several experiments produced less data due to an assortment of instrumental problems and operator errors. A fairly representative experiment is DOY 240, 2000. This experiment consisted of 11 scans each of duration ~26 minutes covering at a wide variety of azimuths and elevations. For ease of comparison between data sets at different elevations both the CEI and WVR data sets have been mapped to zenith.

A time-series of the site-differenced residual phase delay for both the CEI and WVR data for scan 3 is shown in Figure 3. The RMS for the CEI data is 1.7 mm, it is clear that the correlation between the two data sets is strong. The CEI data can be corrected for phase delay fluctuations by subtracting the corresponding WVR data. Figure 4 shows the time-series of the WVR corrected CEI data (calibrated CEI data). The RMS of the calibrated CEI is .5 mm, a factor of three improvement. All other scans in DOY240 were similar to scan 3, by grouping all the scans together a distribution of the CEI residuals before and after WVR correction is shown in Figure 4. The site-difference residual delay RMS is seen to change from ~1.1 mm before the WVR correction to ~.4 mm after the correction.

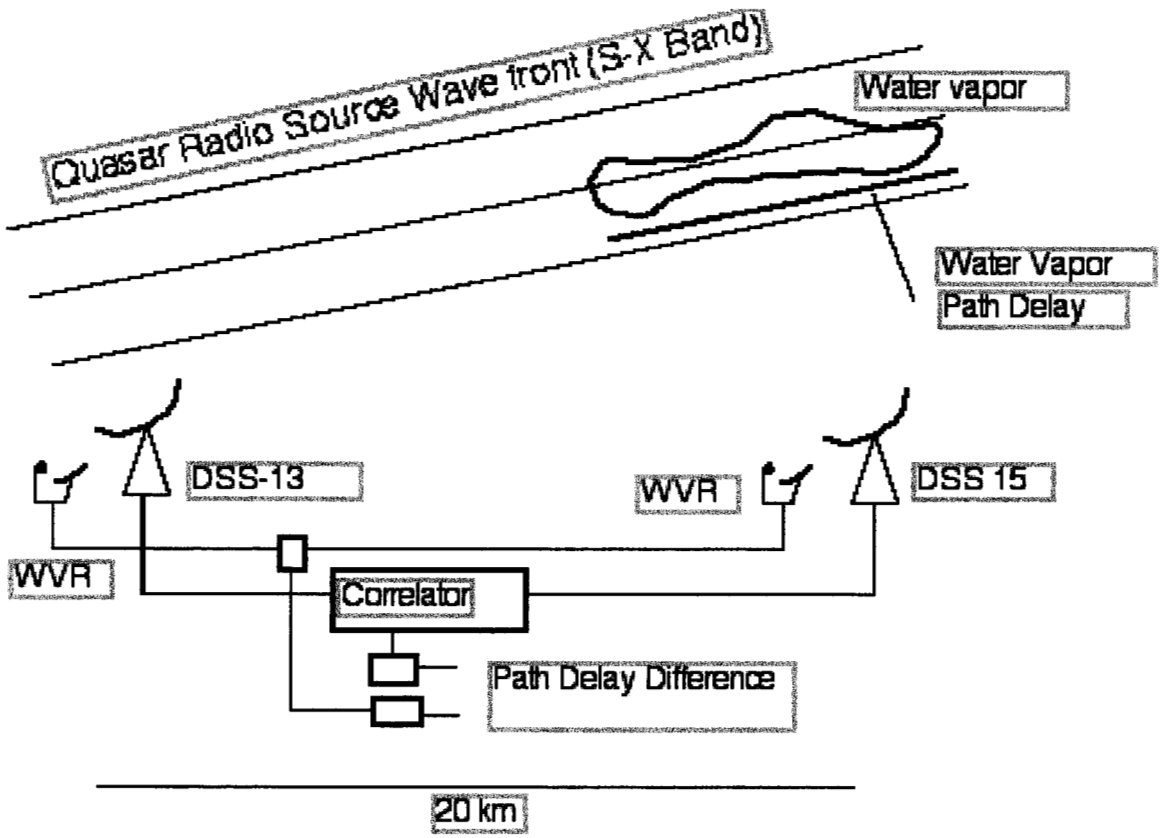

Figure 2. A schematic representation of the WVR/CEI comparison experiments.

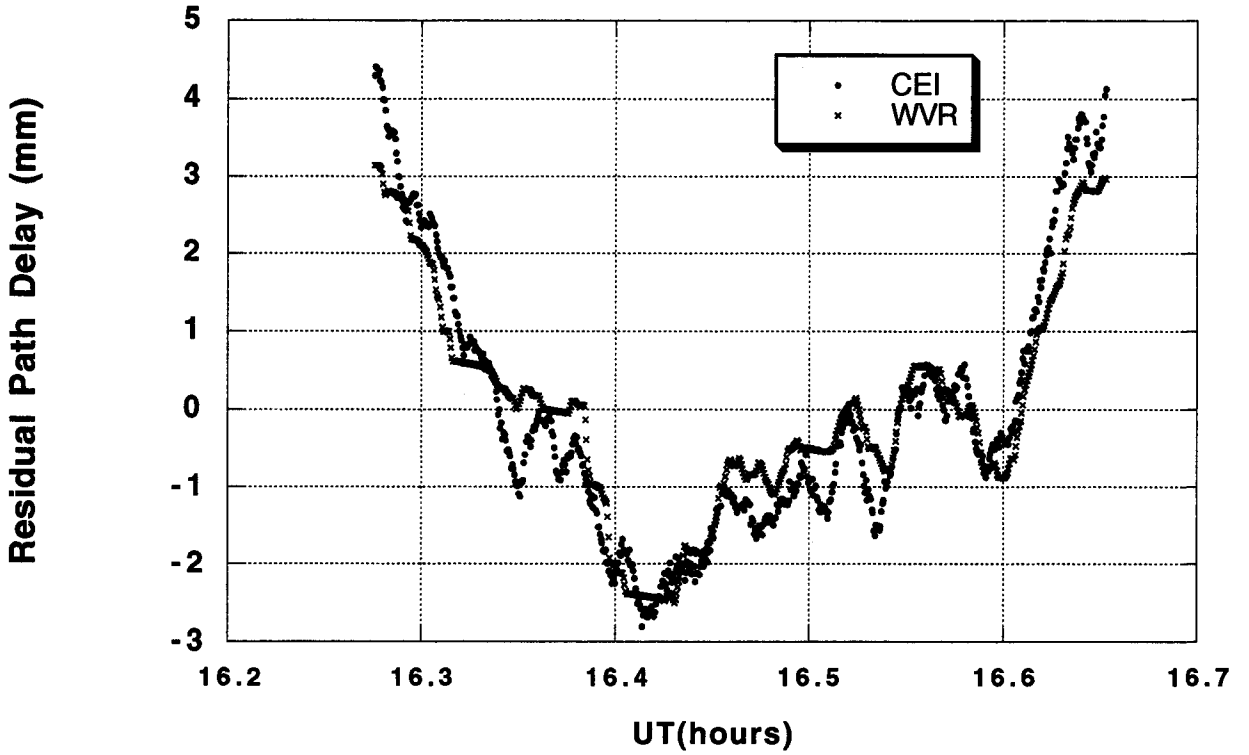

Figure 3. The site differenced, zenith mapped residual delay data from the CEI and WVR for scan 3 on DOY 240, 1999.

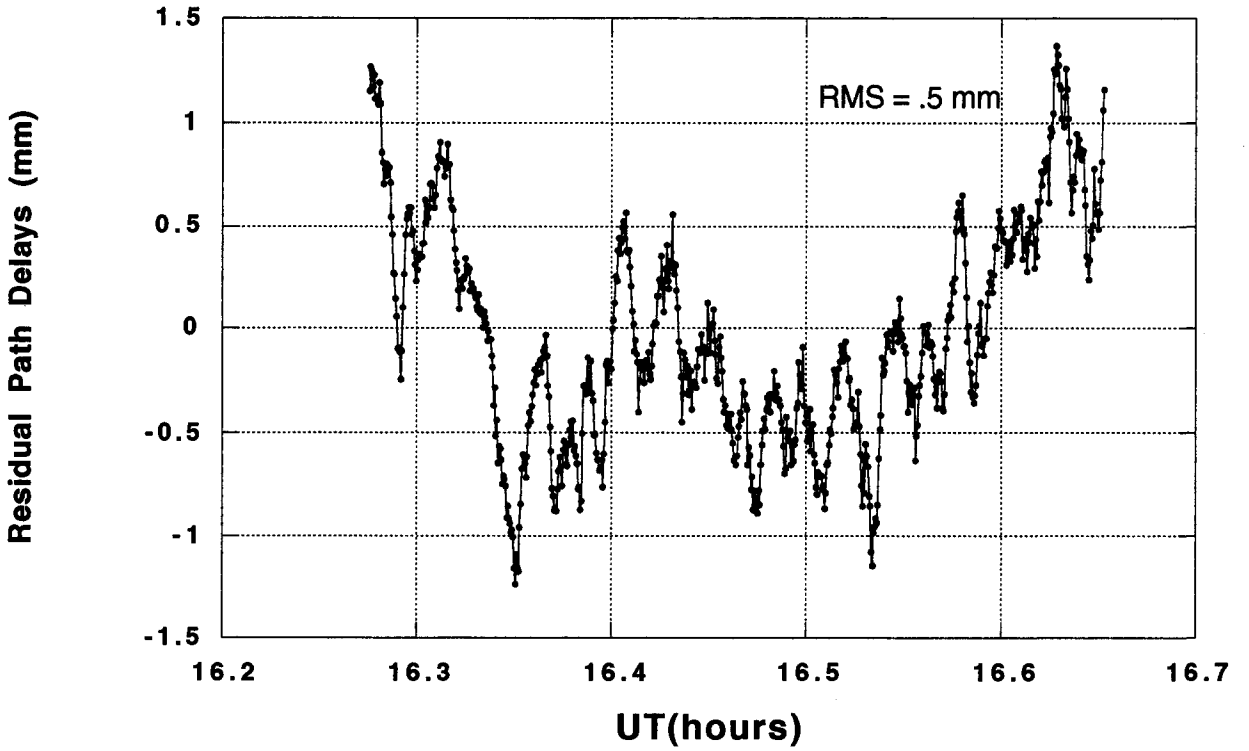

Figure 4. The residual delay of the CEI data, scan 3 on DOY 240 1999, after WVR corrections are applied.

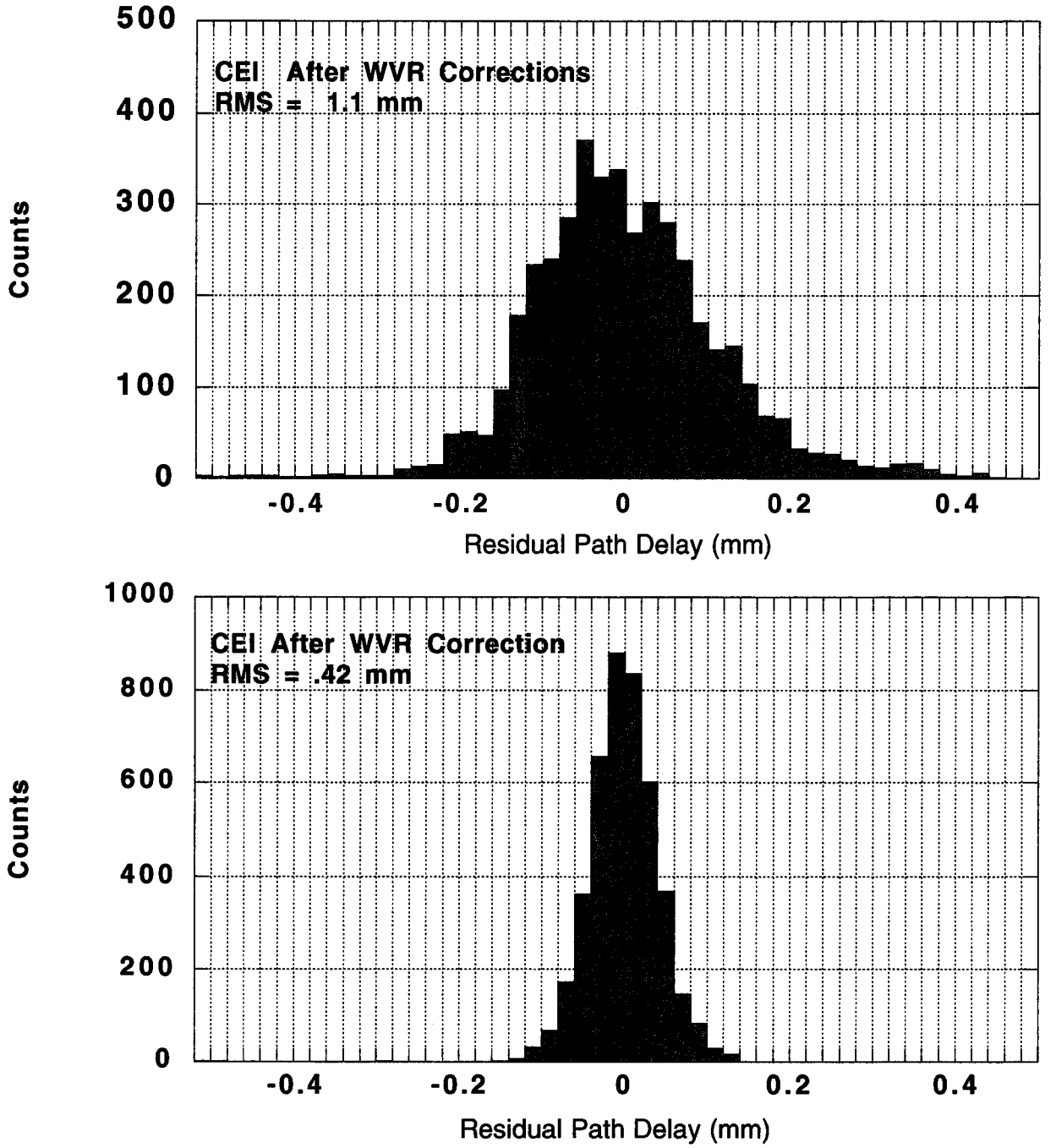

Figure 5. Histograms of the residuals from all scans on DOY 240, 1999. The top histogram shows the residual CEI path delay (RMS = 1.1 mm) and the bottom histogram shows the CEI data after WVR correction (RMS = .42 mm).

By May, 2000 we were able to correct long-term instrumental instability problems enabling WVR-CEI comparison over very long time scales (> 1000 seconds) A representative sample is the time-series data from DOY 138, 2000, shown in Figure 6. The CEI and WVR residual path delays data are seen to track closely. The uncorrected CEI has a RMS = ~ 4.3 mm after WVR correction this is reduced to ~1 mm, a factor of 4 improvement.

Figure 7 plots the Allan standard deviation (ASD) as a function of the sampling time for DOY138. The uncorrected CEI data and WVR data have ASD values that track one another very closely over almost the entire range of sampling times. After the WVR data is used to calibrate the CEI data the ASD is seen to decrease almost a order of magnitude at a sampling time of 1000 seconds. The corrected CEI data shows improvement for all sampling times down to ~10 seconds where it is clear that the correlation between the CEI and WVR data is lost.

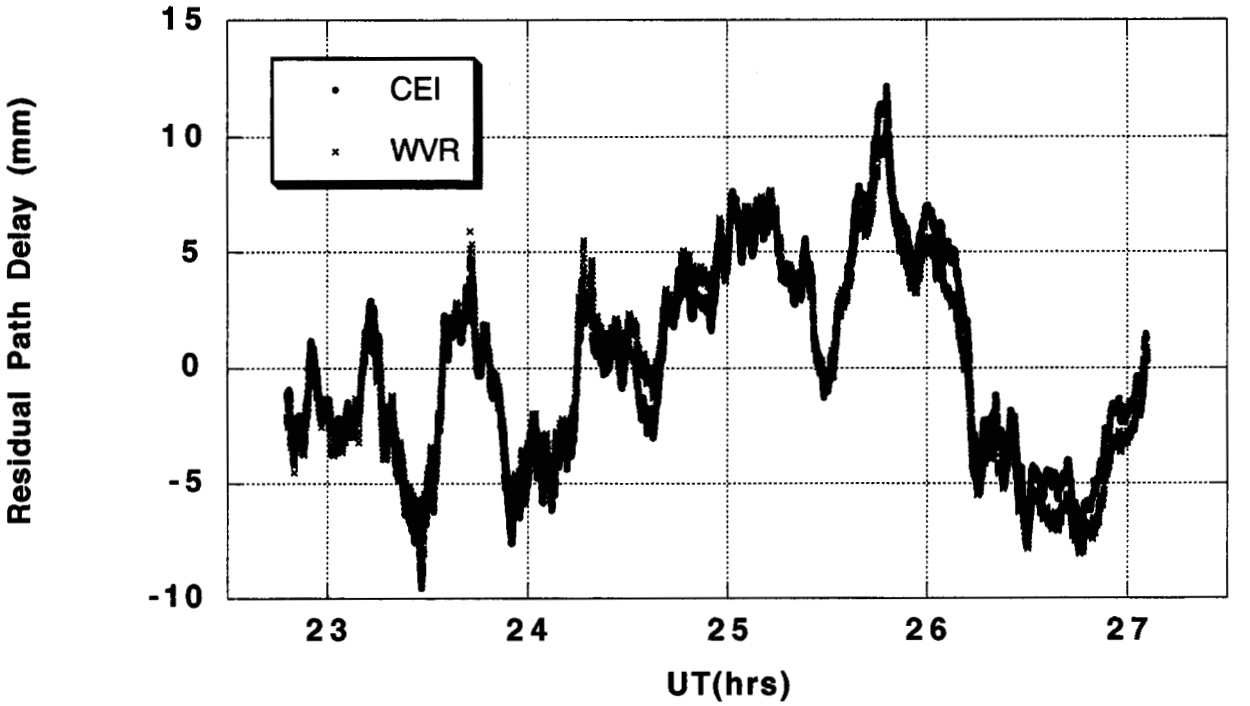

Figure 6. The residual delay of the CEI and WVR for a long scan on DOY 138, 2000. The data is site-differenced, mapped to zenith, and with linear trends removed.

The solid black curve in Figure 7 is the Cassini GWE ASD requirement. For sampling times above 2000 seconds we meet the science objectives. Below sampling times of 1000 seconds we are 2-3 times higher than the requirements. However, this was not unexpected. Early in the design phase the cost performance trade off studies estimated that the ASD less than 1000 seconds would be dominated by the beam offset and mismatch errors. This was deemed acceptable since the majority of the interesting science were in sampling times greater than 1000 seconds.

Discussion

We have described an atmospheric media calibration system which was shown to calibrate out the atmospheric fluctuations down to a Allan standard deviation level of 2×10^{-15} for sampling times greater than 1000 seconds. The Cassini media calibration subsystem was found to meet the science requirements for sampling times greater than 1000 secs. Calibration of the CEI data was found to reduce the residuals by a factor of ~3.

An estimation of the WVR corrected CEI residual phase delay errors, as illustrated in Figure 7, is composed of the quadratic sum of the CEI errors plus the WVR errors. Hence, Figure 7 really is an upper estimate of the WVR residual delay errors. To improve upon our assessment of the WVR performance, the error budget of each measurement technique must be independently examined in greater detail. Work is now under way to critically reevaluate the WVR error budget [precision, stability, beam size, beam offset, beam mismatch, retrieval accuracy] and the CEI error budget [electronic stability, instrumental delay mis-modelling, baseline accuracy].

Acknowledgements

We would like to thank Roger Linfield and Larry Teitelbaum for their helpful discussions on data analysis and John Eric Clark, Charles Snedeker, Lyle Skjerve, Leroy Tanida, the staff of DSS-13, and the Operations crews at the Goldstone Signal Processing Center for the invaluable assistance provided during these operations. The research described in this paper was carried out by the Jet Propulsion Laboratory, California Institute of Technology, under a contract with the National Aeronautics and Space Administration.

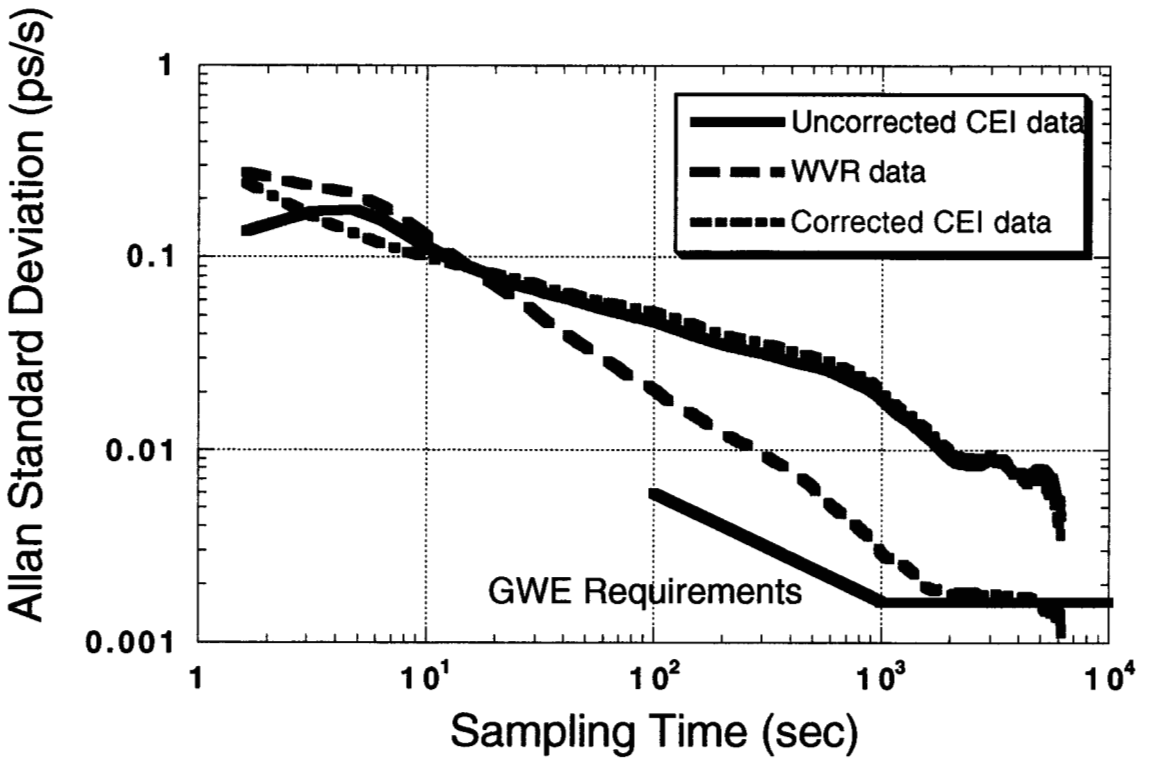

Figure 7. The Allan Standard Deviation plotted as a function of sampling time for the long scan of DOY 138, 2000. The figure shows the CEI residual data, the WVR residual data, the CEI data after WVR corrections, and the requirements for the Cassini GWE.

References

1. Armstrong, J.W., and R.A. Sramek, ``Observations of tropospheric phase scintillations at 5 GHz on vertical paths," Radio Science, 17, pp. 1579 - 1586, Nov. 1982

2. Tinto, M., and J.W. Armstrong ``Spacecraft Doppler tracking as a narrow-band detector of Gravitational Radiation", Phys. Rev. D, 58, 042002, 1998

3 Armstrong, J.W, B. Bertotti, F.B. Estabrook, L. Iess, and H.D. Wahlquist, ``The Galileo/Mars Observer/Ulysses Coincidence Experiment", Proc. of the Second Edoardo Amaldi Conf. on Gravitational Waves, Ed., E. Coccia, G. Pizzella, and G. Veneziano; Edoardo Amaldi Foundation Series, Vol. 4, World Scientific, 1998.

4. Keihm, S.J. ``Water Vapor Radiometer Measurements of the Tropospheric Delay Fluctuations at Goldstone Over a Full Year," TDA Prog. Report, 42-122, p 1-11, 1995

5. Tanner, A.B., ``Development of a high-stability water vapor radiometer," Radio Sci., 33, pp. 449-462, Mar. 1998

6. Resch, G.M., D.E. Hogg, and P.J. Napier, ``Radiometric correction of atmospheric path length fluctuations in interferometric experiments," Radio Sci., 19, pp. 411-422, Jan. 1984

7. Teitelbaum, L.P, R.P. Linfield, G.M. Resch, S.J. Keihm, and M.J. Mahoney, ``A Demonstration of Precise Calibration of Tropospheric Delay Fluctuations With Water Vapor Radiometers," TDA Prog. Report 42-126, pp. 1-8, 1996

8. Resch, G.M., ``Inversion Algorithms for Water Vapor Radiometers Operating at 20.7 and 31.4 GHz," TDA Prog. Report 42-76, pp. 12-26, Oct. 1983

9. Keihm, S.J. and S. Marsh, ``Advanced algorithm and system development for Cassini radio science tropospheric calibration," TDA Prog. Report 42-127, pp. 1-19, 1996

10. Allan, D.W., ``Statistics of Atomic Frequency Standards," Proc. IEEE, 54, No. 2, pp. 221-230, Feb. 1966

11. Lowe, S., ``Theory of Post-Block II VLBI Observable Extraction," JPL Publ. 92-7, 15 July 1992

12. Linfield, R.P., and J. Wilcox, ``Radio metric errors due to mismatch and offset between a DSN antenna beam and the beam of a tropospheric calibration instrument," TDA Prog. Report 42-114, pp. 1-13, 1993

13. Linfield, R.P., ``Error Budget for WVR-based Tropospheric Calibration System," JPL IOM 35.1-96-012, 5 Jun 1996